Anomalously Rapid Tunneling: Charge Transport across Self-Assembled Monolayers of Oligo(ethylene glycol)

Mostafa Baghbanzadeh,[†,#] Carleen M. Bowers,[†,#] Dmitrij Rappoport,[†] Tomasz Żaba,[‡] Li Yuan,[†] Kyungtae Kang,[†] Kung-Ching Liao,[†] Mathieu Gonidec,[†,§] Philipp Rothemund,[†] Piotr Cyganik,[‡] Alan Aspuru-Guzik,[†] and George M. Whitesides[*,†,‖,⊥]

[†]Department of Chemistry and Chemical Biology, Harvard University, 12 Oxford Street, Cambridge, Massachusetts 02138, United States

[‡]Smoluchowski Institute of Physics, Jagiellonian University, Lojasiewicza 11, 30-348 Krakow, Poland

[§]CNRS, Université de Bordeaux, ICMCB, UPR 9048, F-33600 Pessac, France

[‖]Kavli Institute for Bionano Science & Technology, School of Engineering and Applied Sciences, Harvard University, 29 Oxford Street, Cambridge, Massachusetts 02138, United States

[⊥]Wyss Institute of Biologically Inspired Engineering, Harvard University 60 Oxford Street Cambridge, Massachusetts 02138, United States

S *Supporting Information*

ABSTRACT: This paper describes charge transport by tunneling across self-assembled monolayers (SAMs) of thiol-terminated derivatives of oligo(ethylene glycol) ($HS(CH_2CH_2O)_nCH_3$; $HS(EG)_nCH_3$); these SAMs are positioned between gold bottom electrodes and Ga_2O_3/EGaIn top electrodes. Comparison of the attenuation factor (β of the simplified Simmons equation) across these SAMs with the corresponding value obtained with length-matched SAMs of oligophenyls ($HS(Ph)_nH$) and n-alkanethiols ($HS(CH_2)_nH$) demonstrates that SAMs of oligo(ethylene glycol) have values of β ($\beta_{(EG)n} = 0.29 \pm 0.02\ n_{atom}^{-1}$ and $\beta = 0.24 \pm 0.01$ Å^{-1}) indistinguishable from values for SAMs of oligophenyls ($\beta_{(Ph)n} = 0.28 \pm 0.03\ \text{Å}^{-1}$), and significantly lower than those of SAMs of n-alkanethiolates ($\beta_{(CH_2)n} = 0.94 \pm 0.02\ n_{atom}^{-1}$ and $0.77 \pm 0.03\ \text{Å}^{-1}$). There are two possible origins for this low value of β. The more probable involves hole tunneling by superexchange, which rationalizes the weak dependence of the rate of charge transport on the length of the molecules of $HS(EG)_nCH_3$ using interactions among the high-energy, occupied orbitals associated with the lone-pair electrons on oxygen. Based on this mechanism, SAMs of oligo(ethylene glycol)s are good conductors (by hole tunneling) but good insulators (by electron and/or hole drift conduction). This observation suggests SAMs derived from these or electronically similar molecules are a new class of electronic materials. A second but less probable mechanism for this unexpectedly low value of β for SAMs of $S(EG)_nCH_3$ rests on the possibility of disorder in the SAM and a systematic discrepancy between different estimates of the thickness of these SAMs.
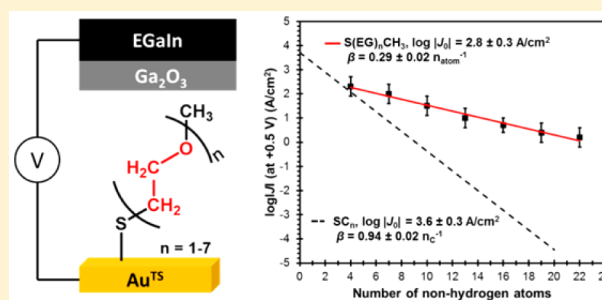
INTRODUCTION

Determining the relationship between the structure of the molecules that make up self-assembled monolayers (SAMs) and the shape of the tunneling barrier that these molecules generate is an area of active research and a part of the broader area of "molecular electronics".[1−14] Our studies have used a junction with the structure M/A-R-T//Ga2O3/EGaIn (where A is the group anchoring the molecules of the SAM to the metal M, R is the backbone of the molecule making up the SAM, T is the terminal group, and EGaIn is a eutectic alloy of gallium and indium. For n-alkanethiolates, for example, A = S, R = $(CH_2)_n$, and T = CH_3 or H, depending on the data being considered. Studies of a range of SAMs based on n-alkanethiolates with different terminal groups (both aliphatic and aromatic), and having the same overall length, have shown remarkably little variation in tunneling current;[15,16] inclusion of groups capable of extended delocalization do lower the barrier to tunneling.[17−20]

This study focuses on the influence of the energy levels of backbone substituents with high-lying occupied orbitals on the height of the tunneling barrier and rates of charge transport. We replaced backbone methylene groups ($-CH_2-$) with oxygen atoms and analyzed the influence of this substitution on the rate of charge transport. The work is complementary to our recently described measurements of charge transport by tunneling across SAMs of short oligoglycines, where the presence of consecutive amide ($-(NHCH_2CO)_n-$) bonds ($n =$

1−5) in a molecule (e.g., $(Gly)_n$) lowered the height of the tunneling barrier relative to length-matched n-alkanethiolates and resulted in a decrease in the measured values of β of the simplified Simmons equation from $\beta_{(CH_2)n} = 0.94\ n_{atom}^{-1}$ to $\beta_{Glyn} = 0.50\ n_{atom}^{-1}$.[21]

We measured rates of charge transport across SAMs containing oligomers of ethylene glycol ($HS(CH_2CH_2O)_nCH_3$; $HS(EG)_nCH_3$, see Figure 1) and compared these rates to rates
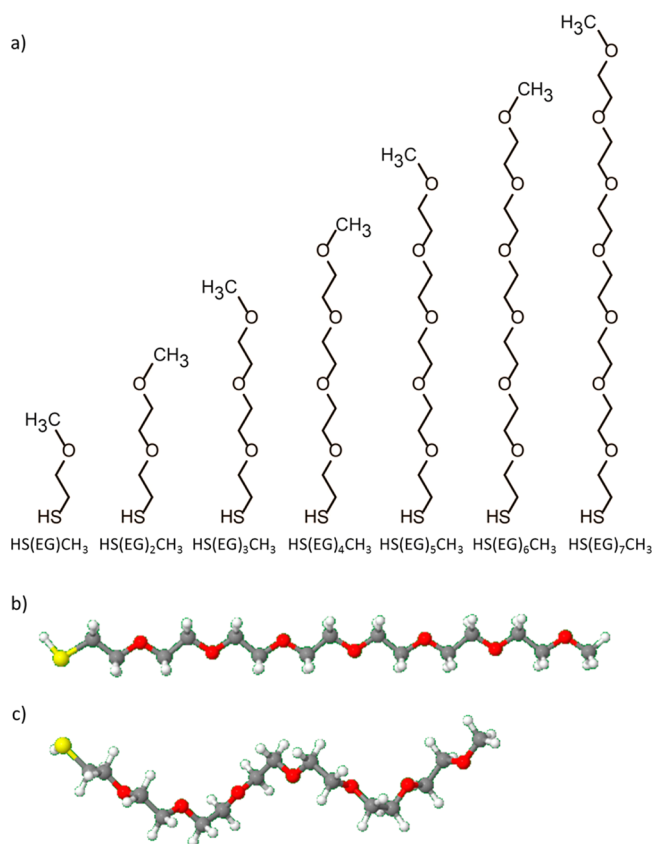

Figure 1. (a) *Trans*-extended representation of mercapto-oligo-(ethylene glycol)s used to form SAMs on Au^{TS}. EG indicates ethylene glycol; n = number of EG units. When the molecules of oligo(ethylene glycol)s are present in a SAM, their structure is noncrystalline and adopts both (b) all-*trans* and (c) all-helix conformations. The depicted conformation was calculated using DFT with B3LYP and def2-SVP functional, resolution-of-the-identity approximation (*RI-J*).

across n-alkanethiolates matched in the number of atoms along the molecular backbone. Modeling of the oligo(ethylene

glycol)s bound to clusters of gold with Density Functional Theory (DFT) predicts a characteristic set of high-lying, delocalized, occupied molecular orbitals, which result from a weak coupling between the lone-pair orbitals on neighboring oxygen atoms in the backbone, and which are absent in n-alkanethiolates. We associate this change in the electronic topography of the tunneling barrier with a decrease in β ($\beta_{(CH_2)n} = 0.94\ n_{atom}^{-1}$ (0.77 Å^{-1})[22] and $\beta_{(EG)n} = 0.29\ n_{atom}^{-1}$, (0.24 Å^{-1})); (here n_{atom} is the number of non-hydrogen atoms—C, N, and O—in the *backbone* of the extended oligomer). Corresponding values of β for four different classes of compounds are summarized in Table 1. Studying charge tunneling across SAMs of oligo(ethylene glycol)s enabled us to establish that the presence of multiple oxygen atoms in the backbone substantially decreases β (relative to SAMs of length-matched n-alkanethiolates). We suggest a rationalization of this decrease based on high-energy, delocalized, occupied MOs formed by superexchange interactions between neighboring oxygen lone-pair orbitals (inferred from DFT results) as being the probable origin of this effect. We discuss, but discount, the possibility that an ambiguity in estimating the thickness of the SAMs of $HS(EG)_nCH_3$ contributes to this estimate of β.

■ BACKGROUND

Charge Transport by Tunneling. Both the orbital energies of the molecules composing the SAM and the interfaces between the SAM and the electrodes influence the rate of charge tunneling.[7,17,23−35] The simplified Simmons equation[36] (eq 1) provides an approximate analytical parametrization of the rate of charge transport across the barrier and predicts an exponential decay in current density with an increasing width of the tunneling barrier, d.[20,37] The value of d is often estimated as the fully extended length (in Å) of the molecule from the anchoring atom bound to the bottom electrode to the distal atom in contact with the Ga_2O_3/EGaIn top electrode, or as the number of repeating units or non-hydrogen atoms in the backbone of the molecule (i.e., the number of carbon atoms in alkanethiols).

$$J(V) = J_0(V) \times 10^{-\beta d/2.303} \tag{1}$$

The proper definition of d for molecules with multiple possible conformations or molecules in disordered SAMs requires an understanding of how rates of tunneling depend on the conformation of the molecules within the SAM. Although much is known about the influence of the conformation of individual molecules on rates of charge transfer,[38−41] less is known about the conformational effects of a *collection* of

Table 1. Summary of Values of β and J_0 for Different Classes of SAMs Measured on Au^{TS} Surfaces[a]

Thiolated SAM on Au^{TS}	Structure	β		J_0 (A/cm^2)[d]
		Å^{-1} [b]	n_{atom}^{-1} [c]	
n-alkane	$HS(CH_2)_nH$	0.77 ± 0.03[e]	0.94 ± 0.03	4.2 ± 0.2
oligophenyl	$HS(Ph)_nH$	0.28 ± 0.03[f]	0.30 ± 0.03[g]	2.7 ± 0.1
oligoglycine	$HS(CH_2)_2(Gly)_nH$	0.45 ± 0.02[h]	0.50 ± 0.02	2.8 ± 0.3
oligo(ethylene glycol)	$HS(EG)_nCH_3$	0.24 ± 0.01	0.29 ± 0.02	2.9 ± 0.1

[a]The ± indicates the error calculated from the standard deviations of the Gaussian mean.[17,21,23] [b]Length (d) calculated in Å for an all-*trans*-extended conformation from the anchoring sulfur atom that chemically contacts to the surface of metal substrates to the distal hydrogen atom. [c]Length (d) calculated based on the number of non-hydrogen atoms in the backbone of the molecule. [d]Values of J_0 are from extrapolation of the linear plots of Figure 2, and are included only for completeness. Because all chains (other than n-alkanes) are heterogeneous, this extrapolation is not meaningful. [e]Ref 23. [f]Ref 17. [g]Number of non-hydrogen atoms for each phenyl ring in the backbone is considered 4. [h]Ref 21.

molecules in the form of a SAM. An important question is, "Does the rate of charge tunneling (assumed to be through bond) depend on the conformation of the molecules through which tunneling occurs?" This problem is one that has not, so far, been solved (or even seriously addressed).

Although the relationship between the structure (molecular and electronic) and shape of the tunneling barrier is not yet completely defined theoretically, the value of β can be used to compare charge transport across different molecular systems. The term $J_0(V)$ is an empirical parameter—obtained through extrapolation—that represents a more substantial (and less easily simplified and interpreted) set of approximations than does β.[22,25,42] The interpretation of J_0 across these SAMs in terms of molecular or molecular-orbital structure—especially for molecules that are heterogeneous in molecular orbital structure (e.g., $(Gly)_n$ and $(EG)_n$)—is not, at present, straightforward, and—for molecules with structures more complex than n-alkanethiols—extrapolation to $d = 0$ will not yield a meaningful value; we therefore focus our analysis on differences in β.

Superexchange Model of Hole Tunneling through Oligo(ethylene glycol)s. The superexchange model[43−45] is a simple atomistic model of tunneling through molecules. This tunneling model predicts an exponential dependence of current density with the length of the molecule and is compatible with both the simplified Simmons equation (eq 1) and empirical calculations.[36] It considers the molecule as a one-dimensional chain of localized orbitals with relatively weak superexchange couplings between them, usually due to interactions between neighboring groups of the same type.[43,44,46] Specifically, in this work, these localized orbitals are oxygen lone pairs in oligo(ethylene glycol)s and peptide bond orbitals in oligo-(glycine)s. The superexchange model was developed by McConnell, Ratner, Nitzan, and co-workers[43−45] to describe charge transport in peptides,[47] and generally provides a qualitative model for electronic conduction (hopping and tunneling) across molecular systems. An independent derivation by E. G. Petrov using the framework of the band model for semiconductors yields the same qualitative result.[48] Due to its conceptual simplicity, the superexchange model also provides an interpretable relationship between the electronic structures of the molecules and their tunneling properties. Perhaps even more importantly, it provides a framework with which to compare different classes of molecules.

We consider a linear chain of n identical units, with one localized orbital per unit, interacting via superexchange with the localized orbitals of the units to its immediate left and right. The (hypothetical) energy of each localized orbital in the absence of the couplings is called the *local orbital energy ε_0*, while the *coupling strength* between orbitals (in units of energy) is denoted as V. Then, the orbital energies ε_j of the MOs resulting from superexchange couplings follow a characteristic splitting pattern,[49]

$$\varepsilon_j = \varepsilon_0 + 2V \cos\left(\frac{j\pi}{n+1}\right), \quad j = 1, ..., n \tag{2}$$

where the index j counts the MOs in the order of increasing energy, n is the total number of units in the chain, and π is the circle constant. The local orbital energy (in the absence of coupling) ε_0 and the coupling strength V are defined above. By equating the predicted orbital energies ε_j with the energies of a set of molecular orbitals (MOs) obtained from DFT

calculations, we are able to extract the determining parameters ε_0 and V.

We have previously applied superexchange model quantitatively to rationalize the rapid rate of tunneling across SAMs of oligoglycines relative to n-alkanethiolates.[21] This model suggested that the substantial couplings between the high-energy occupied orbitals (through which hole tunneling occurs) on the neighboring amide bonds of the oligoglycine molecules were responsible for the experimentally observed rapid (relative to n-alkanethiolates) rate of charge transport.[21] As predicted by Ratner, Nitzan, and co-workers, high tunneling rates are achieved by (i) reducing the energy difference between the local orbital energy ε_0 and the Fermi level of the metal ε_F and (ii) increasing the coupling strength V.[43,44,46] Here, we investigate the applicability of the superexchange model to hole tunneling across SAMs of oligo(ethylene glycol)s and estimate the corresponding values of the parameters ε_0 and V from the orbital energies of the MOs computed by DFT. (The Supporting Information gives details of the DFT calculations and the parameters of the superexchange model.)

Structure of SAMs of Oligo(ethylene glycol)s. We formed thiolated monolayers composed of molecules of oligo(ethylene glycol)s (e.g., $HS(EG)_nCH_3$) and characterized SAMs of them ($n = 1−7$) on surfaces of template-stripped[50] gold (Au^{TS}) using XPS, IRRAS, and static contact angles with water. We relied on XPS to calculate the thickness of the SAMs of $HS(EG)_nCH_3$ on Au^{TS}, and we compared these values of thickness to lengths calculated assuming an all-*trans*-extended conformation and an all-helical conformation (Figure S4). When $n = 2$ and 3, the values of thickness are comparable to the all-*trans*-extended lengths. When $n > 3$, the thicknesses are comparable to the lengths calculated for a helical conformation, suggesting a possible transition in structure with increasing lengths units of ethylene glycol. This suggestion is in agreement with observations from Vanderah et al.[51,52] The results from our structural analysis using IRRAS indicates the formation of *non-crystalline* structures of chemisorbed molecules of ethylene glycol on the surface over the entire range of n. The heterogeneous structural conformation observed in the SAMs of ethylene glycol produce variability in surface coverage and effective film thickness, both of which are lower than the corresponding values for highly ordered SAMs, such as n-alkanethiolates of similar molecular length. The details of our structural analysis are in the Supporting Information.

Meuse and co-workers studied the structural variation and ordering of SAMs of oligo(ethylene glycol)s ($HS(EG)_nCH_3$, where $n = 3−6$, on Au) for potential applications in the generation of protein resistant surfaces. Using reflection−absorption infrared spectroscopy, spectroscopic ellipsometry, and electrochemical impedance spectroscopy,[51,52] their results suggest that monolayers of oligo(ethylene glycol)s on Au are oriented normal to the surface, regardless of the number of units of ethylene glycol (from $n = 3−6$). When $n < 5$, they observed the formation of amorphous structures with some all-*trans* conformations, but little evidence of helical conformations. When $n = 5$ or 6, they observed the formation of highly ordered helical structures.[52]

The upshot of these studies is that there is not uniform agreement in the literature about the conformation of the $(EG)_n$ groups in SAMs. Our XPS work, carried out with modern instruments (Thermo Scientific K-Alpha XPS) with a good signal-to-noise ratio, clearly indicates conformations that extend approximately perpendicular to the surface. Analysis by

ellipsometry indicates thinner monolayers than expected based on calculated lengths, but accurate ellipsometry on these very thin films is difficult,[7,53] and we conclude that the values calculated by XPS are correct for our system.

The influence of *trans*-extended vs helical conformation on the orbital energy is not clear. DFT calculations show that the local orbital energies ε_0 of oxygen lone pairs and the coupling strengths V are not significantly different between the *trans*-extended and all-helical conformations of oligo(ethylene glycol) chains (see Supporting Information).

■ RESULTS AND DISCUSSION

Formation of SAMs. We formed SAMs of thiol-terminated oligo(ethylene glycol)s on template-stripped gold substrate (Au^{TS})[54] by immersing the Au^{TS} substrates in a 3 mM ethanolic solution[51] of thiol, purged with nitrogen, for 24 h at room temperature. Immediately prior to electrical measurements, we rinsed the SAMs with ethanol and removed the residual ethanol by evaporation under a gentle stream of nitrogen. We estimated the thickness for SAMs of oligo(ethylene glycol)s using both fixed-angle XPS and angle-resolved XPS techniques. The results of thicknesses for SAMs of $HS(EG)_nCH_3$ (n = 2−7) on Au^{TS} using angle-resolved XPS and fixed-angle XPS analysis are summarized in Table S2. Figure S4 compares the experimental thicknesses (measured by angle-resolved XPS) with calculated lengths for both all-*trans* and helical conformations. The thickness values of $HS(EG)_nCH_3$ are comparable with the all-*trans* lengths when n = 2 and 3. When n > 3, the thicknesses are comparable with the lengths of the helical conformations. Further surface characterization using infrared reflection absorption spectroscopy (IRRAS) identified the formation of multiple conformational phases (helical, all-*trans*, and amorphous) in the monolayer for all lengths of $HS(EG)_nCH_3$ (n = 3−7). This result is compatible with the XPS data.

Measuring Current Densities by Tunneling. Table S6 summarizes the results for charge tunneling across SAMs of oligo(ethylene glycol)s and *n*-alkanethiolates on Au^{TS} using what we call "selected"[55] conical tips of $Ga_2O_3/EGaIn$; we have described this type of junction in detail previously.[22] Measurements of J(V) at forward and reverse biases (±0.5 V and ±1.0 V) produced nearly symmetrical profiles with rectification ratios ($r = |J(+V)/J(−V)|$) ≤ ~4 for both SAMs of alkanethiolates and SAMs of oligo(ethylene glycol)s on gold. Using our junction, this value of r is not large enough to be interpreted and not statistically distinguishable from 1.

Our studies were carried out with junctions of the form $Au^{TS}SR//Ga_2O_3/EGaIn$. Experimental studies of charge transport across SAMs of alkanethiolates using this junction and others have been described extensively,[22,56,57] and the data from these studies on gold serve as standards to which we compare changes in rates of charge transport with changes in molecular structure for other series of compounds (Table 1). (In the study described here, the structural change is the substitution of oxygen for a methylene group). We measured charge transport by tunneling across the SAMs in the low-bias regime (V = ± 0.5 V), where β is independent of the applied bias.[36,58] For all systems, Gaussian mean values of $\langle \log|J| \rangle$ decreased linearly with increasing d (estimated by assuming a *trans*-extended conformation for the $(EG)_n$ group). Given the complexity in the structure of SAMs of oligo(ethylene glycol)s, we also approximated d, the distance between the electrodes, as the number of non-hydrogen atoms in the backbone of the molecules.

Linear regression analyses of the values of $\langle \log|J| \rangle$ versus d yielded values of β for SAMs of oligo(ethylene glycol)s on gold substrates (Figures 2 and S9). The value of β for SAMs of
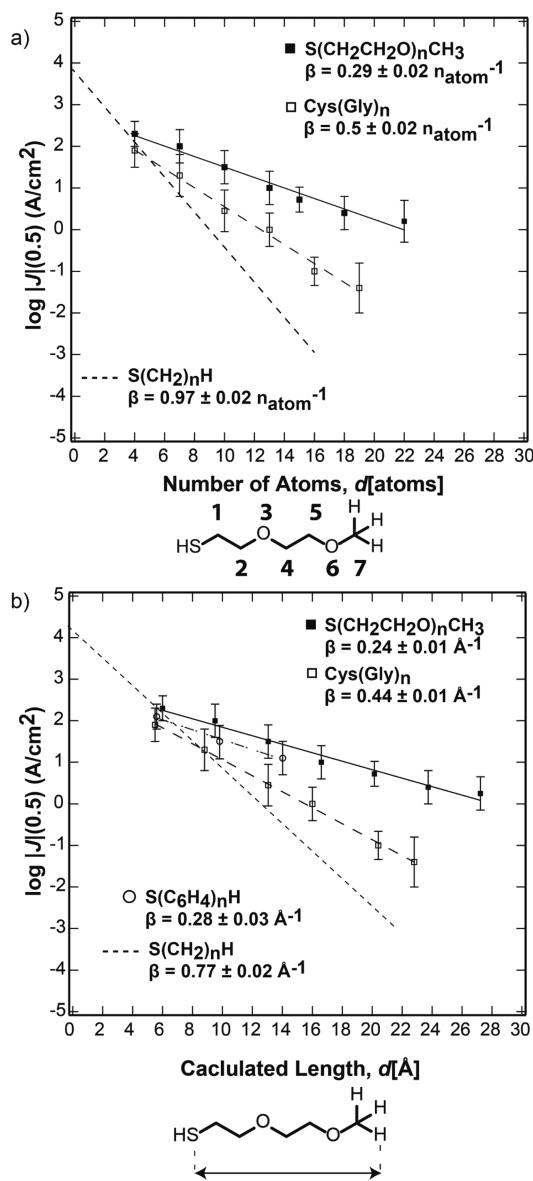
Figure 2. Plot of the Gaussian mean values of $\log|J|$ at +0.5 V versus (a) the number of non-hydrogen atoms in the backbone of the molecule, starting with carbon next to the sulfur atom and counting to the final non-hydrogen atom (for example, number of atoms for $HS(EG)_2CH_3$ is 7), and (b) the calculated length in Å for an all-*trans*-extended conformation from the anchoring sulfur atom that chemically contacts to the surface of metal substrates to the distal hydrogen atom. The solid line indicates data collected for oligo(ethylene glycol)s, where n is the number of ethylene glycol units in $HS(EG)_nCH_3$. The error bars represent the standard deviation of the Gaussian mean values (for details of measurements see the Supporting Information).

$HS(EG)_nCH_3$ was $\beta_{(EG)_n} = 0.29 \pm 0.02$ n_{atom}^{-1} when assuming d to be the number of non-hydrogen atoms in the backbone of molecule; this value is much lower than that measured for SAMs of *n*-alkanethiolates on gold ($\beta_{(CH_2)_n} = 0.94$ n_{atom}^{-1}).[57] We also approximated d as the length of the *trans*-extended molecule from the anchoring atom to the distal hydrogen atom to calculate β in units of Å^{-1}; this analysis yields $\beta_{(EG)_n} = 0.24$

Å^{-1} (Figure 2b), which is comparable to that describing tunneling across SAMs of oligophenyls on gold ($\beta_{(CH_2)_n}$ = 0.28 Å^{-1}).[17] Figure S9 shows analyses of $\langle log|J|\rangle$ versus d, where d is approximated as the film thickness (measured with angle-resolved XPS); this method gives $\beta_{(EG)_n}$ = 0.54 Å^{-1}. Table 1 summarizes β and log|J_0| values for SAMs of oligo(ethylene glycol)s and compares them with those of other known systems.
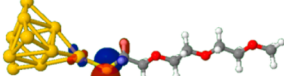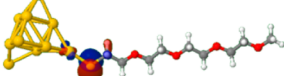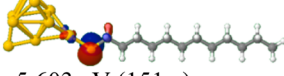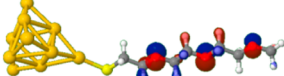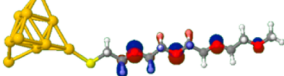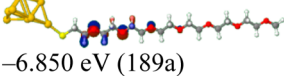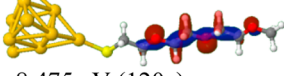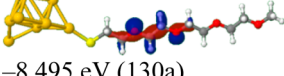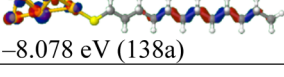
The disorder in the molecular structure of SAMs of oligo(ethylene glycol)s, and the probable involvement of multiple conformations, make it difficult to estimate the width of the tunneling barrier (d) unambiguously. Moreover, it makes the values of rates of charge transport less certain than those estimated for SAMs of well-ordered n-alkanethiols. Despite this heterogeneity in structure, there is a clear linear dependence of $\langle log|J|\rangle$ on the value of d, when d is approximated either as the number of non-hydrogen atoms along the backbone (Figure 2a) or by estimation for a *trans*-extended conformation (Figure 2b). This observation suggests that—for charge transport by hole tunneling across SAMs of oligo(ethylene glycol)s—the atomic length of molecules (e.g., the number of atoms in the chain) dominates the width of the tunneling barrier, and not the defects of conformation or regularity of packing of these molecules in the SAM.

To further examine the influence of the structure of SAMs of oligo(ethylene glycol)s on current density, we compared the current density across SAMs of HS(EG)$_n$CH$_3$ on Au^{TS} with (i) HS(EG)$_n$CH$_3$ (n = 3, 5) on template-stripped silver (Ag^{TS}) and (ii) HOOC(EG)$_n$CH$_3$[59] (n = 2, 3) on Ag^{TS} (Figures S7 and S8). Changing the substrate from gold to silver and the anchoring group from thiol to carboxylate influences the structure of the SAM.[60] Despite the change in substrate and anchoring group, molecules of oligo(ethylene glycol), with equivalent number of repeating units, produce comparable current densities. The similar current densities between the three classes of SAMs on silver and gold support the conclusion that the length of the oligo(ethylene glycol) molecule—rather than the details of its conformation—defines the width of the tunneling barrier.

The difference in rates of charge transport between SAMs of ethylene glycol and SAMs of alkanethiolate is unexpected, given that both molecular systems (structures having both C−C and C−O bonds) have electronic transitions that occur only at wavelengths less than 200 nm,[61,62] with corresponding HOMO−LUMO gaps for both types of structures of about 7−8 eV, as calculated in the gas phase (Tables S10 and S11).[62]

Computed Molecular Orbital Structures. The differences in the structures of the molecular orbitals from DFT calculations provide a rationalization for the change in β. DFT calculations using the Becke three-parameter hybrid exchange-correlation functional (B3LYP)[63] and split-valence basis sets (def2-SVP)[64] (see Supporting Information for full computational details) indicate that the HOMO is localized on the sulfur anchoring atom in both alkanethiolates and thiolate-terminated oligo(ethylene glycol)s bound to clusters of gold; the energy of this orbital for the two structures is indistinguishable (∼ −5.6 eV, Table 2). Also, the high-lying MOs located on the C−C σ bonds of the backbone are similar for both structures (∼ −8.0 eV, Table 2). The notable differences in the computed molecular orbital structures are due to oxygen lone-pair orbitals, which give rise to a set of high-energy occupied MOs delocalized over the oligo(ethylene

Table 2. Orbital Energies (eV) for the Spin-Up (alpha) Molecular Orbitals Localized on (A) the Sulfur Atom, (B) the Lone Pair of Oxygen and the C−H bond, and (C) the C−C Bond for Thiol-Terminated Oligo(ethylene glycol) and Dodecanethiolate on Au$_{10}$ Clusters[a]

A. Cluster	MO, S alpha
Au$_{10}$S(CH$_2$CH$_2$O)$_3$CH$_3$	−5.672 eV (143a)
Au$_{10}$S(CH$_2$CH$_2$O)$_4$CH$_3$	−5.678 eV (155a)
Au$_{10}$S(CH$_2$)$_{11}$CH$_3$	−5.603 eV (151 a)
B. Cluster	**MO, O/C–H alpha**
Au$_{10}$S(CH$_2$CH$_2$O)$_3$CH$_3$	−6.817 eV (141a)
Au$_{10}$S(CH$_2$CH$_2$O)$_4$CH$_3$	−6.833 eV (153a)
Au$_{10}$S(CH$_2$CH$_2$O)$_7$CH$_3$	−6.850 eV (189a)
C. Cluster	**MO, C–C alpha**
Au$_{10}$S(CH$_2$CH$_2$O)$_3$CH$_3$	−8.475 eV (120a)
Au$_{10}$S(CH$_2$CH$_2$O)$_4$CH$_3$	−8.495 eV (130a)
Au$_{10}$S(CH$_2$)$_{11}$CH$_3$	−8.078 eV (138a)

[a]The results for the whole series of compounds (Au/S-(CH$_2$CH$_2$O)$_n$CH$_3$; n = 3−7) are shown in the Supporting Information.

glycol) backbone. The highest-energy MO for each oligo-(ethylene glycol) chain length is shown in Table 2.

Our crucial observation is that the orbital energies of these MOs formed from oxygen lone-pair orbitals and computed using DFT follow the functional relationship predicted by the superexchange tunneling model (eq 2) with good accuracy. By fitting the orbital energies ε_j of these MOs in oligo(ethylene glycol)s (S(EG)$_n$CH$_3$, n = 3−7) bound to clusters of gold (Au$_{10}$S(EG)$_n$CH$_3$) against their orbital indices j and the chain lengths n, we are able to extract the determining parameters of the superexchange model: the (hypothetical) energy of an isolated oxygen lone-pair orbital (local orbital energy) ε_0 = (−6.99 ± 0.007) eV and the coupling strength V = (−0.09 ± 0.005) eV between the oxygen lone pairs at neighboring

ethylene glycol units (see Table 3). The Supporting Information describes the DFT calculations and the fit to the superexchange model in more detail.

Table 3. Summary of the Superexchange Tunneling Parameters, ε_0 and V, for Oligo(ethylene)-, Oligo(propylene)-, and Oligo(butylene glycol)s

cluster	ε_0 (eV)	V (eV)
$Au_{10}S(CH_2CH_2O)_nCH_3$	-6.99 ± 0.007	-0.09 ± 0.005
$Au_{10}S(CH_2CH_2CH_2O)_nCH_3$	-6.91 ± 0.004	-0.09 ± 0.003
$Au_{10}S(CH_2CH_2CH_2CH_2O)_nCH_3$	-6.85 ± 0.010	-0.05 ± 0.010

Superexchange Model of Tunneling in Oligo(Ethylene Glycol)s. The oxygen lone pairs have a (hypothetical) orbital energy of ~ -7.0 eV in the absence of superexchange interactions; this value is still well below the HOMO energy of ~ -5.6 eV. The effect of the superexchange coupling is, however, to create a set of high-energy, delocalized, occupied MOs which extend along the molecular backbone (unlike the HOMO which is localized predominately on the sulfur atom; Table 2). We note that the interaction between *occupied* orbitals (oxygen lone pairs) does not fit the textbook picture of bond formation due to overlap between an occupied and a vacant orbital. The coupling strength of the interaction between oxygen lone pairs ($|V| \approx 0.1$ eV) is less than 5% of the bond energies of typical bonds (2−4 eV) and does not contribute to the stabilization (or destabilization) of the oligo(ethylene glycol) chains. Rather, it is due to a relatively weak quantum mechanical (exchange) effect between the electrons occupying the oxygen lone-pair orbitals on the neighboring ethylene glycol units.

This proposal for an electronic basis for rapid hole tunneling is similar to that which we proposed for hole tunneling across SAMs of oligoglycine,[21] and the two studies are thus mutually reinforcing, especially since they involved two classes of molecules with very different, molecular and electronic structures. Studying the electronic structures of oligoether chains of different composition gives us an opportunity to investigate how the distance between the oxygen atoms along the molecular backbone influences the molecular electronic parameters relevant to hole tunneling. To this end, we compared the results of the DFT calculations for oligo(ethylene glycol)s bound to a $(Au)_{10}$ cluster with those for oligo(1,3-propanediol) ($Au_{10}S(CH_2CH_2CH_2O)_nCH_3$; $n = 3-5$) and oligo(butane-1,4-diol) ($Au_{10}S(CH_2CH_2CH_2CH_2O)_nCH_3$; $n = 3-5$) similarly bound to gold ($Au_{10}S(CH_2CH_2CH_2O)_nCH_3$; $n = 1-3$). Surprisingly, the coupling strength in the series of gold-bound oligo(1,3-propanediol)s is indistinguishable from that in oligo(ethylene glycol)s, despite the larger distance between the oxygen atoms: $\varepsilon_0 = (-6.91 \pm 0.004)$ eV, $V = (-0.09 \pm 0.003)$ eV (see Table 3). Four $-CH_2-$ units between the oxygen atoms are necessary to reduce the coupling strength to a value that is effectively "non-interacting"; the series of gold-bound oligo(1,4-butanediol) give $\varepsilon_0 = (-6.85 \pm 0.01)$ eV and $V = (-0.05 \pm 0.01)$ eV (Figures S12 and S13 and Table 3).

CONCLUSION

The interaction of multiple oxygen atoms along the backbone of SAMs of oligo(ethylene glycol)s ($HS(EG)_nCH_3$ ($n = 1-7$)) influences rates of charge transport by hole tunneling. The value of β of the simplified Simmons equation (Table 1) is lower for SAMs of oligo(ethylene glycol)s on gold than for

SAMs of *n*-alkanethiolates on gold and comparable to that of oligophenylenes $(-C_6H_4-)_n$. The oxygen atoms in the backbone interact in a way that results in high-lying, delocalized molecular orbitals at ~ -7 eV that arise from superexchange coupling between neighboring lone-pair orbitals on oxygen. (The orbitals localized on sulfur and on the C−C bonds are unaffected, and their energies on molecules of oligo(ethylene glycol)s and alkanethiolates are indistinguishable.) The strength of the interactions between nearest oxygen atoms in oligo-(ethylene glycol)s and oligo(1,3-propanediol)s is indistinguishable; this observation suggests that similar measurements in rates of charge transport would be observed.

The strength of the interactions between nearest oxygen atoms calculated using the superexchange model also rationalizes the high tunneling conductivity observed for oligoglycines.[21] Charge tunneling across SAMs of oligoglycine is comparable to SAMs of oligophenyls[21] and correlates with the presence of high-lying, delocalized, occupied orbitals formed from the π orbitals of the peptide bonds.

The rapid rate of tunneling across SAMs of both oligo-(ethylene glycol) and oligoglycine suggests that these classes of molecules should be considered as members of a new class of organic electronic materials: good conductors by tunneling, but poor conductors by electronic drift. The conductivity of these compounds is also relevant to questions concerning the ability of biopolymers (both proteins and nucleic acids) to support charge tunneling. Moreover, the observation that calculated interactions between neighboring amide bonds correlate with experimentally observed rates of charge transport suggests that the superexchange model will be useful as a predictive tool in designing molecules with tunneling barriers engineered for potential and topography.

ASSOCIATED CONTENT

Ⓢ Supporting Information

The Supporting Information is available free of charge on the ACS Publications website at DOI: 10.1021/jacs.7b02770.

Detailed experimental procedure and histograms of current densities (PDF)

AUTHOR INFORMATION

Corresponding Author

*gwhitesides@gmwgroup.harvard.edu

ORCID Ⓘ

Mostafa Baghbanzadeh: 0000-0001-7678-1681

Piotr Cyganik: 0000-0001-6131-4618

Alan Aspuru-Guzik: 0000-0002-8277-4434

George M. Whitesides: 0000-0001-9451-2442

Author Contributions

#M.B. and C.M.B. contributed equally to this work.

Notes

The authors declare no competing financial interest.

■ REFERENCES

(1) Nitzan, A.; Ratner, M. A. *Science* **2003**, *300*, 1384−1389.
(2) Thompson, D.; Nijhuis, C. A. *Acc. Chem. Res.* **2016**, *49*, 2061−2069.
(3) McCreery, R. L.; Yan, H.; Bergren, A. *J. Phys. Chem. Chem. Phys.* **2013**, *15*, 1065−1081.
(4) Perrin, M. L.; Burzuri, E.; van der Zant, H. S. *J. Chem. Soc. Rev.* **2015**, *44*, 902−919.
(5) Metzger, R. M. *Chem. Rev.* **2015**, *115*, 5056−5115.
(6) Xiang, D.; Wang, X.; Jia, C.; Lee, T.; Guo, X. *Chem. Rev.* **2016**, *116*, 4318−4440.
(7) Vilan, A.; Aswal, D.; Cahen, D. *Chem. Rev.* **2017**, *117*, 4248−4286.
(8) Fracasso, D.; Muglali, M. I.; Rohwerder, M.; Terfort, A.; Chiechi, R. C. *J. Phys. Chem. C* **2013**, *117*, 11367−11376.
(9) Sangeeth, C. S. S.; Wan, A.; Nijhuis, C. A. *J. Am. Chem. Soc.* **2014**, *136*, 11134−11144.
(10) Sayed, S. Y.; Fereiro, J. A.; Yan, H. J.; McCreery, R. L.; Bergren, A. J. *Proc. Natl. Acad. Sci. U. S. A.* **2012**, *109*, 11498−11503.
(11) Bergren, A. J.; McCreery, R. L.; Stoyanov, S. R.; Gusarov, S.; Kovalenko, A. *J. Phys. Chem. C* **2010**, *114*, 15806−15815.
(12) Yan, H.; Bergren, A. J.; McCreery, R. L. *J. Am. Chem. Soc.* **2011**, *133*, 19168−19177.
(13) Bergfield, J. P.; Ratner, M. A. *Phys. Status Solidi B* **2013**, *250*, 2249−2266.
(14) McCreery, R. L.; Bergren, A. J. *Adv. Mater.* **2009**, *21*, 4303−4322.
(15) Yoon, H. J.; Shapiro, N. D.; Park, K. M.; Thuo, M. M.; Soh, S.; Whitesides, G. M. *Angew. Chem., Int. Ed.* **2012**, *51*, 4658−4661.
(16) Yoon, H. J.; Bowers, C. M.; Baghbanzadeh, M.; Whitesides, G. M. *J. Am. Chem. Soc.* **2014**, *136*, 16−19.
(17) Bowers, C. M.; Rappoport, D.; Baghbanzadeh, M.; Simeone, F. C.; Liao, K. C.; Semenov, S. N.; Zaba, T.; Cyganik, P.; Aspuru-Guzik, A.; Whitesides, G. M. *J. Phys. Chem. C* **2016**, *120*, 11331−11337.
(18) Salomon, A.; Böcking, T.; Gooding, J. J.; Cahen, D. *Nano Lett.* **2006**, *6*, 2873−2876.
(19) Wold, D. J.; Haag, R.; Rampi, M. A.; Frisbie, C. D. *J. Phys. Chem. B* **2002**, *106*, 2813−2816.
(20) Ho Choi, S.; Kim, B.; Frisbie, C. D. *Science* **2008**, *320*, 1482−1486.
(21) Baghbanzadeh, M.; Bowers, C. M.; Rappoport, D.; Zaba, T.; Gonidec, M.; Al-Sayah, M. H.; Cyganik, P.; Aspuru-Guzik, A.; Whitesides, G. M. *Angew. Chem., Int. Ed.* **2015**, *54*, 14743−14747.
(22) Simeone, F. C.; Yoon, H. J.; Thuo, M. M.; Barber, J. R.; Smith, B.; Whitesides, G. M. *J. Am. Chem. Soc.* **2013**, *135*, 18131−18144.
(23) Bowers, C. M.; Liao, K. C.; Zaba, T.; Rappoport, D.; Baghbanzadeh, M.; Breiten, B.; Krzykawska, A.; Cyganik, P.; Whitesides, G. M. *ACS Nano* **2015**, *9*, 1471−1477.
(24) Sepunaru, L.; Refaely-Abramson, S.; Lovrincic, R.; Gavrilov, Y.; Agrawal, P.; Levy, Y.; Kronik, L.; Pecht, I.; Sheves, M.; Cahen, D. *J. Am. Chem. Soc.* **2015**, *137*, 9617−9626.

(25) Sangeeth, C. S.; Wan, A.; Nijhuis, C. A. *Nanoscale* **2015**, *7*, 12061−12067.
(26) Vilan, A.; Cahen, D. *Chem. Rev.* **2017**, *117*, 4624−4666.
(27) Wierzbinski, E.; Yin, X.; Werling, K.; Waldeck, D. H. *J. Phys. Chem. B* **2013**, *117*, 4431−4441.
(28) Xie, Z.; Bâldea, I.; Oram, S.; Smith, C. E.; Frisbie, C. D. *ACS Nano* **2017**, *11*, 569−578.
(29) Song, H.; Kim, Y.; Jang, Y. H.; Jeong, H.; Reed, M. A.; Lee, T. *Nature* **2009**, *462*, 1039−1043.
(30) Bruot, C.; Hihath, J.; Tao, N. *J. Nat. Nanotechnol.* **2012**, *7*, 35−40.
(31) Guo, C. L.; Yu, X.; Refaely-Abramson, S.; Sepunaru, L.; Bendikov, T.; Pecht, I.; Kronik, L.; Vilan, A.; Sheves, M.; Cahen, D. *Proc. Natl. Acad. Sci. U. S. A.* **2016**, *113*, 10785−10790.
(32) Kumar, S.; van Herpt, J. T.; Gengler, R. Y. N.; Feringa, B.; Rudolf, P.; Chiechi, R. C. *J. Am. Chem. Soc.* **2016**, *138*, 12519−12526.
(33) Song, P.; Yuan, L.; Roemer, M.; Jiang, L.; Nijhuis, C. A. *J. Am. Chem. Soc.* **2016**, *138*, 5769−5772.
(34) Petrov, E. G.; Zelinskyy, Y. R.; May, V.; Hanggi, P. *J. Chem. Phys.* **2007**, *127*, 084709.
(35) Petrov, E. G.; Shevchenko, Y. V.; May, V. *Chem. Phys.* **2003**, *288*, 269−279.
(36) Simmons, J. G. *J. Appl. Phys.* **1963**, *34*, 1793−1803.
(37) Choi, S. H.; Frisbie, C. D. *J. Am. Chem. Soc.* **2010**, *132*, 16191−16201.
(38) Verhoeven, J. W. *Pure Appl. Chem.* **1990**, *62*, 1585−1596.
(39) Lauteslager, X. Y.; van Stokkum, I. H. M.; van Ramesdonk, H. J.; Bebelaar, D.; Fraanje, J.; Goubitz, K.; Schenk, H.; Brouwer, A. M.; Verhoeven, J. W. *Eur. J. Org. Chem.* **2001**, *2001*, 3105−3118.
(40) Oevering, H.; Paddon-Row, M. N.; Heppener, M.; Oliver, A. M.; Cotsaris, E.; Verhoeven, J. W.; Hush, N. S. *J. Am. Chem. Soc.* **1987**, *109*, 3258−3269.
(41) Oliver, A. M.; Craig, D. C.; Paddon-Row, M. N.; Kroon, J.; Verhoeven, J. W. *Chem. Phys. Lett.* **1988**, *150*, 366−373.
(42) Jiang, L.; Sangeeth, C. S. S.; Wan, A.; Vilan, A.; Nijhuis, C. A. *J. Phys. Chem. C* **2015**, *119*, 960−969.
(43) Kosloff, R.; Ratner, M. A. *Isr. J. Chem.* **1990**, *30*, 45−58.
(44) Nitzan, A. *Annu. Rev. Phys. Chem.* **2001**, *52*, 681−750.
(45) McConnell, H. *J. Chem. Phys.* **1961**, *35*, 508.
(46) Joachim, C.; Ratner, M. A. *Proc. Natl. Acad. Sci. U. S. A.* **2005**, *102*, 8801−8808.
(47) Gray, H. B.; Winkler, J. R. *Proc. Natl. Acad. Sci. U. S. A.* **2005**, *102*, 3534−9.
(48) Petrov, E. G. *Int. J. Quantum Chem.* **1979**, *16*, 133−152.
(49) Salem, L. *The Molecular Orbital Theory of Conjugated Systems* W. A. Benjamin: New York, 1996.
(50) Weiss, E. A.; Chiechi, R. C.; Kaufman, G. K.; Kriebel, J. K.; Li, Z. F.; Duati, M.; Rampi, M. A.; Whitesides, G. M. *J. Am. Chem. Soc.* **2007**, *129*, 4336−4349.
(51) Vanderah, D. J.; Valincius, G.; Meuse, C. W. *Langmuir* **2002**, *18*, 4674−4680.
(52) Vanderah, D. J.; Arsenault, J.; La, H.; Gates, R. S.; Silin, V.; Meuse, C. W.; Valincius, G. *Langmuir* **2003**, *19*, 3752−3756.
(53) Palik, E. D. *Handbook of Optical Constants of Solids*; Academic Press: Orlando, fL, 1985.
(54) Weiss, E. A.; Kaufman, G. K.; Kriebel, J. K.; Li, Z.; Schalek, R.; Whitesides, G. M. *Langmuir* **2007**, *23*, 9686−9694.
(55) Bowers, C. M.; Liao, K.-C.; Yoon, H. J.; Rappoport, D.; Baghbanzadeh, D.; Simeone, F. C.; Whitesides, G. M. *Nano Lett.* **2014**, *14*, 3521−3526.
(56) Engelkes, V. B.; Beebe, J. M.; Frisbie, C. D. *J. Am. Chem. Soc.* **2004**, *126*, 14287−14296.
(57) Baghbanzadeh, M.; Simeone, F. C.; Bowers, C. M.; Liao, K. C.; Thuo, M.; Baghbanzadeh, M.; Miller, M. S.; Carmichael, T. B.; Whitesides, G. M. *J. Am. Chem. Soc.* **2014**, *136*, 16919−16925.
(58) Simmons, J. G. *J. Appl. Phys.* **1963**, *34*, 2581−2590.
(59) Liao, K.-C.; Yoon, H. J.; Bowers, C. M.; Simeone, F. C.; Whitesides, G. M. *Angew. Chem., Int. Ed.* **2014**, *53*, 3889−3893.

(60) Love, J. C.; Estroff, L. A.; Kriebel, J. K.; Nuzzo, R. G.; Whitesides, G. M. *Chem. Rev.* **2005**, *105*, 1103−1169.

(61) Cheng, T. L.; Chuang, K. H.; Chen, B. M.; Roffler, S. R. *Bioconjugate Chem.* **2012**, *23*, 881−899.

(62) Costner, E. A.; Long, B. K.; Navar, C.; Jockusch, S.; Lei, X.; Zimmerman, P.; Campion, A.; Turro, N. J.; Willson, C. G. *J. Phys. Chem. A* **2009**, *113*, 9337−9347.

(63) Becke, A. D. *J. Chem. Phys.* **1993**, *98*, 5648−5652.

(64) Weigend, F.; Ahlrichs, R. *Phys. Chem. Chem. Phys.* **2005**, *7*, 3297−3305.